

I-Detect: Life Detection Under Debris in Disaster Zones

Poola, Lakshmi ; John, Luis Henrik; Godkhindi, Shrutkirthi S. ; Reddy, Preetham ; Rao, Deeksha P.; Prabhakar, T. V.; Venkatesha Prasad, R.

DOI

[10.1109/COMSNETS59351.2024.10427472](https://doi.org/10.1109/COMSNETS59351.2024.10427472)

Publication date

2024

Document Version

Final published version

Published in

Proceedings of the 2024 16th International Conference on COMmunication Systems & NETworkS (COMSNETS)

Citation (APA)

Poola, L., John, L. H., Godkhindi, S. S., Reddy, P., Rao, D. P., Prabhakar, T. V., & Venkatesha Prasad, R. (2024). I-Detect: Life Detection Under Debris in Disaster Zones. In *Proceedings of the 2024 16th International Conference on COMmunication Systems & NETworkS (COMSNETS)* (pp. 345-352). (Communication Systems and Networks and Workshops. Proceedings). IEEE. <https://doi.org/10.1109/COMSNETS59351.2024.10427472>

Important note

To cite this publication, please use the final published version (if applicable). Please check the document version above.

Copyright

Other than for strictly personal use, it is not permitted to download, forward or distribute the text or part of it, without the consent of the author(s) and/or copyright holder(s), unless the work is under an open content license such as Creative Commons.

Takedown policy

Please contact us and provide details if you believe this document breaches copyrights. We will remove access to the work immediately and investigate your claim.

Green Open Access added to TU Delft Institutional Repository

'You share, we take care!' - Taverne project

<https://www.openaccess.nl/en/you-share-we-take-care>

Otherwise as indicated in the copyright section: the publisher is the copyright holder of this work and the author uses the Dutch legislation to make this work public.

l-Detect: Life Detection under Debris in Disaster Zones

Lakshmi Poola*, Luis Henrik John[†], Shrutkirthi S. Godkhindi*, Preetham Reddy*, Deeksha P Rao*,
T V Prabhakar*, R Venkatesha Prasad[†]

*Department of Electronic Systems Engineering, Indian Institute of Science, Bengaluru, India

[†]Delft University of Technology, Delft, Netherlands

*{lakshmipoola, shrutkirthig, preethamg, deeksharao, tvprabs}@iisc.ac.in

[†]l.john@erasmusmc.nl, [†]r.r.venkateshaprasad@tudelft.nl

Abstract—The recent spate of natural disasters such as earthquakes and floods destroyed buildings and caused loss of lives. Many times, the loss of life is attributed to slow response and not being able to reach the survivors. In such scenarios, the staggering number of deaths in the aftermath of a disaster can be reduced if information about survivors under debris is available to first responders and rescue workers. Large-scale destruction of roads and other communication infrastructure makes it hard to deploy advanced technologies for life detection. We explore the possibility of using low-cost, low-power, short-range communication technologies to assist rescue personnel in locating life under debris. We have designed and prototyped a thermopile-based sensor and communication device that provides information about the presence of survivors. The system weighs under 20 gm and costs US\$30 per unit. The device can easily be fitted on battery-powered toy bugs and robots that can autonomously maneuver under the debris. We have proposed three simple algorithms, which together detect humans with 100% to 88% accuracy for 0.5 to 4.5 m range with fewer false alarms. Our evaluation shows that the detection is robust enough under several harsh ambient conditions, temperature ranges as well and partial exposure of the human body.

Index Terms—thermopile, life-detection, infrared, low cost, debris.

I. INTRODUCTION

Natural disasters such as earthquakes and floods as well as incidents like nuclear accidents occur leading to large-scale destruction of infrastructure and loss of several thousands of lives. Hundreds of people go missing under fully and partially collapsed buildings. For instance, the recent Morocco earthquake left 500 residences and several commercial buildings razed to the ground. Several remote places were inaccessible, due to the damages caused to the road infrastructure [1]. Similarly, Libya floods left four major bridges collapsed, and 25% of the city was inaccessible. In Raigad, India, floods damaged many buildings and hundreds of people were trapped under debris.

When such natural disasters occur, communication systems, navigation systems and electrical distribution systems get affected causing entire townships to plunge into darkness. Amidst this large-scale confusion and despair, the hope to find survivors looms large. It is a race against time to rescue humans buried under building debris. People in the locality, risk their lives and look for survivors in these unstable structures

using naive methods and existing tools. For search and rescue missions locating survivors buried under the pile is difficult. The task of locating survivors continues to be an unsolved problem even with the advent of modern technology. For instance, transporting cranes and other equipment is difficult due to lack of road infrastructure. Furthermore, using such equipment in these operations is time-consuming. For every miscalculated search operation, more lives are lost than that could have been rescued.

In this work, we propose *l*-Detect (Life Detection platform), a low-cost, low-power and low infrastructure sensor platform to detect life under building debris. The design components of *l*-Detect are carefully selected so that it is easily available, affordable, disposable, rapidly producible and easily set up. Our *l*-Detect incorporates a low-cost, thermopile sensor setup, which could be easily deployable and maneuverable under debris. The device is easily mountable on small robots, toy cars, miniature bugs, lightweight quadcopters, etc. Further, on-board processing is enabled to conserve power, without compromising on performance and detection. The detection results are communicated using Bluetooth low energy (BLE). This work aims to cover all the required steps in sensing and data processing. The robotics and the miniature bugs that can be controlled remotely (or move autonomously) used to carry *l*-Detect as a payload is beyond the purview of this paper. However, we discuss some aspects briefly without providing any detailed investigation. The main contributions of this work are listed below:

- ① We design *l*-Detect platform which is light-weight, low cost (under US\$30) and has a low form-factor. We characterized and calibrated the thermopile sensor for thermal imaging.
- ② We evaluated *l*-Detect in different scenarios, under *in-situ* conditions, under different ambient temperature.
- ③ A Machine Learning (ML) model is built to detect humans buried under the debris as well as to classify different human postures.

II. RELATED WORKS

A myriad of solutions are proposed in the literature to detect human presence under harsh conditions. For instance, air-scenting dog units capable of picking up a scent from humans are reported in [2]. Radar-based techniques have also

TABLE I: Comparison of the related works

| Work | Sensor used | Algorithm | bulky | indoor | Mis-detection level |
|---|--|---|-------|--------|---------------------|
| A pedestrian detection system [3] | thermopiles and radars | pattern classification, DST | yes | no | high |
| Human detection using thermopiles [4] | 8×1 thermopile | thresholding, normalizing | no | yes | moderate |
| Heat mapping for improved victim detection [5] | uEYE and web camera, laser range finder, thermopiles | linear interpolation and component analysis | yes | yes | high |
| Detection of surviving humans [6] | PIR and IR sensor, Cameras | neural networks | yes | no | moderate |
| Snake-like robots to search victim under debris [7] | tactile sensor, vision sensor, 12 cameras, 60 small lights | real time map construction, MMI | yes | no | NA |
| Human detection and geolocalization for rescue missions [8] | GPS receiver, PC104 barometric altitude sensor | thermal and colour imagery, geolocation mapping | yes | no | low |
| Human body tracking [9] | CCD, thermal camera | sensor fusion, SBT | no | no | moderate |
| Earthquake survivor detection [10], [11] | doppler radars | EMD analysis, bioradar | yes | no | moderate |
| <i>l</i> -Detect | 8×8 Grid-EYE thermopile | local maxima, DCT variance | no | yes | low |

found attention in recent years owing to their penetration capability through obstructing objects. Human bio-signals [12] are modulated on the radar signal, which is then used to train the ML model to recognize survivors under the debris. Frequency of life signal (FMAS) is proposed in [11], where the radar signal is subjected to SSS-transform, to obtain a high resolution, high signal-to-noise ratio, and time-frequency map to detect humans behind the wall. In the microwave detection system presented in [13], survivors are detected using reflected microwaves that are modulated by human movements, including breathing and heartbeat. Apart from being an expensive technology, a significant limitation of using microwaves is the effect of the background noise created by the environment and operators. Wi-Vi, a WiFi-based through-wall human detection technique is proposed in [14]. Wi-Vi can detect objects and humans moving behind opaque structural obstructions. This applies to 0.2 m concrete walls, 0.15 m hollow walls, and 4 cm solid wooden doors. However, there are many operational difficulties in a disaster zone. In [15], the system can localize a human and corresponding posture with the assistance of objects surrounding the human. In [16], a thermal imaging sensor system mounted on a UAV is used for human detection. Parallel image processing algorithms, filters, etc., were used to extend the range up to 2 km. The importance of thermal imagery for face recognition and detection without being affected by external factors such as illumination is discussed in [17]. However, this work mainly focuses on the comparison of several computationally intensive techniques. Thermopile-based PIR sensors are an excellent choice to identify pedestrians, but differentiating them from clutter (lamp posts, cars and many other objects) is a challenge [3]. In [18], PIR sensors are used for human detection where a trigger ensures that an image of the human is captured using a low-cost web camera. An IR sensor mounted on a robotic platform is used for obstacle detection. Thermopiles are used for people counting in doorways and pedestrian detection from a mobile robot using an 8×1 thermopile array sensor [4]. The algorithm

normalises and compares the measured temperature with respect to a threshold to distinguish between a person standing in front of the sensor and a person passing by. A dynamic threshold is used to account for the changing skin temperature of a person, which is affected by ambient temperature. In [19], the Grid-EYE sensor, which is essentially an infrared array sensor, is used to detect human presence in a room. The Grid-EYE's sensitivity and its appealing features are demonstrated. Grid-EYE is used for detecting human occupancy and distance monitoring during the COVID-19 pandemic and was reported in [20] and [21]. Having established the efficacy of the Grid-EYE sensor, we also find there are novel robotic solutions to carry the Grid-EYE sensor. Although such solutions are out of scope in this work, we surveyed three novel crawler solutions [7], [22], and [23]. In particular, the development of snake-like robots [22] that can be employed to search for human life under different kinds of debris surfaces is interesting and worth mentioning. A snapshot of the existing solutions and the proposed system is presented in Table I.

From the literature elaborated above, we arrived at a few features for our proposed platform. The proposed system needs to be low-cost, lighter, robust, compact, and energy-efficient. We believe that it is easy to integrate our low-cost hardware on existing robot platforms such as Robbie [5]. The goal is to assist first responders in detecting life with a high success probability.

III. SENSOR SELECTION

Some of the factors addressed while designing *l*-Detect are: **1** *Sensor requirement*: the sensor should be compact, operate in zero lux conditions and reliably detect life under debris. **2** *Processing and computation*: data processing algorithms to detect humans have to be lightweight, and yet work efficiently on low-power platforms. **3** *Usage*: the system has to be designed such that it is easy to operate and to find the trapped survivors under debris. The thermal sensor selection and

thermal imaging feature for our *l*-Detect platform is explained in the following section.

A. Sensor selection

1) *Selecting a suitable sensor*: The sensors can be selected based on the application and several other crucial factors like cost, energy consumed, form factor, resolution, detection range and field of view (FoV). Thermal sensors have several of these features and thermopile's digital output can be directly used for processing. There are a variety of thermal sensors available in the market. Table II lists the different thermal sensors available in the market that are suitable for human detection.

TABLE II: Comparison of different thermal sensors available in the market suitable for human detection

| Parameter | Grid-EYE | 4×4 OD6T | Fluke Ti10 |
|-----------------------------|--------------|------------|---------------|
| Cost (USD \$) | 30 | 54 | 900 |
| Resolution (W×H) | 8×8 | 4×4 | 640×480 |
| Form Factor (mm) (L×H×W) | 11.6×4.3×8 | 14×3.75×18 | 150×270×130 |
| Operating Temperature | -20 to 100°C | 5 to 50°C | -20 to 250 °C |
| Weight (gm) | 10 | 10 | 1200 |
| Range (m) | 5 | 3-3.5 | NA |
| Field of View (°) | 60×60 | 45×45 | 23×17 |

From Table II, Panasonic Grid-EYE costs about 30 USD, and clearly has an advantage over 4×4 Omron OD6T (54 USD) in terms of cost, resolution and range. Commercial IR cameras from Fluke are top-of-the-line available in the market. The Fluke Ti10 IR [24] camera captures thermal images with a resolution of 400×300 pixels, and is highly sensitive to temperature variations. The large form factor and high cost make it a hard choice for our application.

B. Thermal imaging principle

Seebeck described the thermo-electric effect as a voltage generated proportional to the temperature difference between two thermo-electrically dissimilar metals, such as copper and bismuth, and results in a thermocouple [25]. According to the Stefan-Boltzmann law, the total power radiated by an object P_{obj} is given by Equation 1, where A_{obj} is the surface area, σ is the Stefan-Boltzmann constant, ϵ is its emissivity and T_{obj} is its thermodynamic temperature.

$$P_{obj} = A_{obj}\epsilon\sigma T_{obj}^4. \quad (1)$$

The net radiation P_{rad} received by the thermopile is equal to the difference between the power radiated by the object and the power radiated by the thermopile itself as given by Equation 2.

$$P_{rad} = K'\sigma(\epsilon_{obj}T_{obj}^4 - \epsilon_{TP}T_{TP}^4). \quad (2)$$

The constant $K' = K \sin^2 \frac{\phi}{2}$ is dependent on the field-of-view ϕ of the sensor, K is the Boltzmann constant [26], T_{obj}

is the temperature of the object and T_{TP} is the temperature of the thermopile. The voltage generated by the thermopile is proportional to P_{rad} [4]. This allows temperature measurement of distant objects when the ambient temperature of the thermopile's reference junction is known. Because the thermopile operates on a temperature difference, it becomes selective to infrared radiation. This concept is the central technology for our platform.

C. Decimation

Since Fluke Ti10 has a good resolution, we captured thermal images and decimated them to different pixel resolutions to evaluate the minimum resolution required to detect life under debris. The images were taken from distances of 1.5 m to 2 m from the subject and distributed to 64×64, 16×16, 8×8 and 4×4 pixel resolutions. Fig. 1 shows the decimated images and a brief comparison with the 8×8 Grid-EYE images. After analysing and comparing all the decimated images, we found that a thermal image of 8×8 pixel resolution is sufficient to detect human presence. Further from Fig. 1d and 1e, it can be seen that the thermal images from Grid-EYE are comparable with the Fluke IR images. Hence, we have opted for Grid-EYE thermal sensors to detect human beings amidst the debris and rubbles in calamity-struck areas. The idea is also that less pixel data can help in easy data transmission and also more privacy awareness.

IV. *l*-DETECT HARDWARE AND SENSOR CHARACTERISATION

A. Sensor hardware setup

The *l*-Detect setup comprises of the following hardware: **nRF52840** chip is programmed to receive the sensed data from the thermal sensor, process it and transmit it to the user. nRF52840 is an ultra-low power System on Chip (SoC), with an Arm Cortex-M4 processor, with 1 MB flash program memory, and 256 kB RAM on board, to support the sensor data processing. It also supports Bluetooth Low Energy (BLE), and a 2.4 GHz wireless system integrating a multiprotocol 2.4 GHz transceiver [27]. We use BLE to send information about the processed data to the user. The thermal sensor needs an input voltage of 5 V to operate, whereas the SoC requires 3.3 V. A power management using **LTC3105** DC-DC Converter is incorporated on our platform. **Grid-EYE** is a compact Infra-Red (IR) sensor and is composed of 64 individual thermopile elements arranged in an 8×8 matrix. The integrated lens in Grid-EYE focuses the infrared in the FoV onto the sensor elements. This generates voltage differences between electrodes of individual thermopile elements, which is converted to temperature information. Grid-EYE's integrated ASIC performs the core functions to enable the sensor's performance such as pixel readouts, analog amplification, analog to digital conversion, sensitivity correction, correction for temperature effects, and digital readout [28]. A **battery** pack consisting of two 1.65 V AA batteries powers the hardware. The *l*-Detect can also be powered by connecting it to the robotic platform. Fig. 3 shows the *l*-Detect system powered

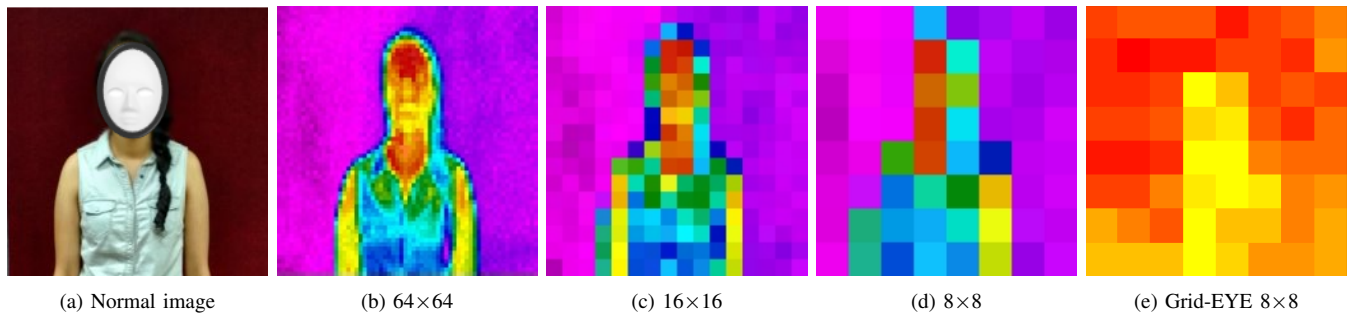


Fig. 1: Series of thermal images from a subject captured from a distance of 1.5 m - 2 m. The original image is captured on the Fluke Ti10 IR camera and decimated to 64×64 , 16×16 , and 8×8 resolutions. The 8×8 Fluke Ti10 image is compared with the Grid-EYE sensor image

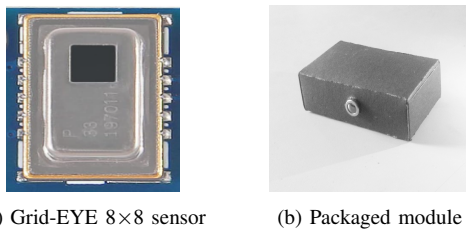


Fig. 2: *I*-Detect platform

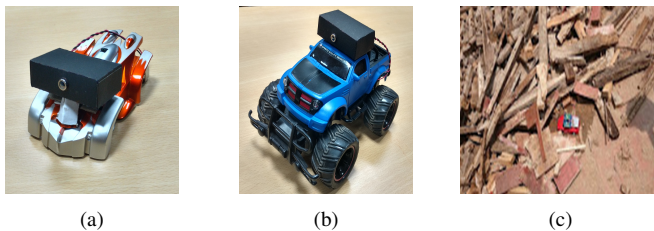


Fig. 3: (a) and (b) *I*-Detect mounted on different robotic cars, (c) Robo car in debris

from the remote controlled car's battery on which it was mounted. The microcontroller and the DC-DC converter are embedded on a single printed circuit board and enclosed in a module shown in Fig. 2b.

B. Sensor characterization

The Grid-EYE is characterised under different environmental conditions to meet the primary objective of survivor detection. The colour map of the thermal images is scaled individually to provide the largest possible contrast. Thus even a slight spatial temperature variation would help in contour detection. The colour gradient ranges used are from black (low temperatures), over red and yellow, to white (high temperatures). 15 frames of thermal images from the sensor are considered to do the detection.

Reference junction: The thermopiles rely on the temperature of a reference junction to interpret the Seebeck voltage accurately. Collocated with this junction is a thermocouple used for ambient temperature measurement. For reliable measurement, the thermal time constant and its effect have to be considered.

We found that the first 3 to 4 frames have to be discarded before using them for the measurement. To verify our claims, we heated the sensor from behind with a hot air gun and observed that consistent and reliable readings from all the pixels were obtained after the 4th frame. The system settled down to provide the right temperature values as soon as the back and front sides of the sensor reached an equilibrium.

Pixel energy diffusion: Since the Grid-EYE thermal sensor has a 60° viewing angle, the thermal radiations get diffused into adjacent pixels and this obfuscates the presence of humans at a particular spot. However, the pixel diffusion reduces as the sensor moves closer to the target subject. For instance, when the head of the person fits completely into one pixel, the diffusion no more affects the detection possibility.

Skin temperature: While the skin temperature in most cases is expected to be above the ambient temperature, the measurement sometimes can appear to be lower due to several external parameters such as distance of the sensor to the object, FoV, and resolution of the sensor. In the case of human detection, it measures the skin temperature, which varies relative to the ambient temperature, although not linearly. Additionally, different body parts radiate different amounts of heat; the head and the torso being the most prominent of all. The Grid-EYE does not measure the core body temperature of objects but rather measures the surface temperature.

Ambient noise: Noise is a major factor that affects the detection process. The noise can be external, caused due to the environment, or internal, caused by the sensor due to the reference junction. Depending on the objects that are present in the FoV of the Grid-EYE, it can be difficult to distinguish a human from a heat source available close to the sensor because human signature diffuses into the background. To assess the ambient noise, a point of reference is chosen. In the case of the Grid-EYE, this reference can be the onboard temperature sensor, which is located in the proximity of the reference junction of the thermopile matrix. Eliminating noise was a challenging part and it was dealt with in the detection algorithm discussed in the next section.

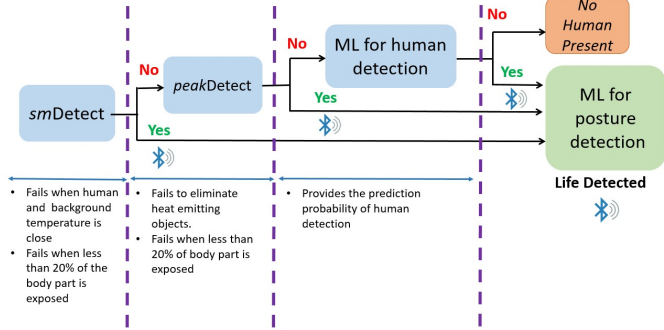


Fig. 4: Human detection model in the *l*-Detect platform

V. *l*-DETECT SENSING AND DETECTION METHODOLOGY

In this work, our approach is to focus on accurate human detection under debris. The human body can be partially buried or obstructed and the postures are restricted to sleeping, sitting, standing and crouching. The proposed algorithm suggests the presence of a human by estimating the person's skin temperature.

A. Algorithms

We noticed that the detection accuracy is highest if the body is fully exposed and if the robotic platform carrying the *l*-Detect could go closer to the person. We have developed significantly lightweight algorithms that can categorize as close to the ground truth as possible. Our *l*-Detect system would communicate only in cases when it recognises the human contour with high probability. We have three sets of algorithms – *smDetect*, *peakDetect* and a classification model. *smDetect* uses simple *second moments* (SM) of the pixel data over 15-20 frames to cancel out the noise and locate the pixel where we could find the thermal projection of a person. By default *smDetect* results are used for human detection and in the event when the result is close to the noise floor, *peakDetect* is used. In either case, the final step is to apply the classification algorithm to weed out false positives. Fig. 4 captures all the detection algorithms and methodologies to detect human life.

1) *smDetect*: We found empirically that an average of 15 SMs are sufficient to detect human life. To establish the threshold, the algorithm takes all the 64 pixel values, and ambient temperature and returns the SM values. Further, we repeat this operation about 10 - 15 times with a small delay between the frames to remove the clutter noise emitted from other warm objects in the surroundings. It is safe to assume that in the initial 15 frames that were collected, humans were not present. We declare the presence of humans if the mean SM is greater than the specified threshold. The working of the SM algorithm is given in Algorithm 1. The limitation of this algorithm is its inability to detect human life whenever the temperature is close to the background temperature. For example, at a temperature of 32°C, both humans and the

background are at the same temperature. We also found the algorithm has limited efficacy when less than 20% of the body is exposed under the debris.

Algorithm 1 *smDetect* Algorithm

- 1: Input: First 15 frames F_i , $i = \{1, 2, \dots, 15\}$;
- 2: Compute second moment for each frame, SM_i , $\forall i = 1, 2, \dots, 15$ frames;
- 3: Threshold: $Th = \text{mean}(SM_i)$;
- 4: Collect new mean SM_r , for every set of 15 running frames;
- 5: **if** $SM_r > 2 \times Th$ **then**
- 6: send "Found" signal from BLE to the user;
- 7: **else if** $2 \times Th < SM_r < 2 \times Th$ **then**
- 8: "More Processing Required" to the user;
- 9: **else**
- 10: $Th = 0.5 \times Th + 0.5 \times SM_r$ (update the noise frames)
- 11: **end if**
- 12: GOTO Step 4

2) *peakDetect*: This algorithm is enabled automatically when the SM value is close to the detection threshold. *peakDetect* works on IDCT-FFT by identifying prominent peaks that indicate the presence of humans. We found that 21 frames are required to reliably establish human presence. Algorithm 2 explains *peakDetect* to identify peaks. In each

Algorithm 2 *peakDetect* Algorithm

- 1: Input: 21 frames of F_j , where $F = \{x_1, x_2, \dots, x_{64}\}$, $j = \{1, 2, \dots, 21\}$;
- 2: Compute $F_j^m = \{x_1, x_2, \dots, x_{64}\} - \text{mean}(F_j)$, for 21 frames;
- 3: Take $Y_j = \text{abs}(\text{FFT}(\text{IDCT}\{F_j^m\}))$, where Y_j is an array of 21 samples;
- 4: Find peak, $P = \max\{Y_j\}$;
- 5: Count C_j for each frame, F_j , samples in $Y_j > 0.75P$, $j = \{1, 2, \dots, 21\}$;
- 6: **if** $C_j > 5$ **then**
- 7: Mark frame $M_j = 0$;
- 8: **else**
- 9: Mark frame $M_j = 1$;
- 10: **end if**
- 11: **if** $\sum_j M_j > 11$ **then**
- 12: send "Found" signal to the user;
- 13: **else**
- 14: GOTO Step 1 for next 21 frames;
- 15: **end if**

frame, we subtract the mean pixel value from the individual pixels.

B. Classification model

To eliminate false negatives from *peakDetect* we have further incorporated ML model. A false negative is the case when the *peakDetect* gives 'no life' even when life is present.

Such a scenario occurs when the body part exposed is less than 20%. Among the several available multi-class classifiers such as Naive Bayes, KNN, Decision Tree and SVM, we found that Support Vector Machine (SVM) provided the best accuracy. The SVM parameters like kernel selection such as the Radial Basis Function, 'C' and ' γ ' (evaluated for 2, and 0.0625 respectively), were determined using "grid search" with 5-fold cross validation [29].

VI. EVALUATION AND RESULTS

To study the efficacy of our algorithms, we conducted a series of experiments in harsh conditions that *l*-Detect would possibly encounter. Since ambient temperatures vary over the day, we collected extensive data throughout the day. Furthermore, evaluation was considered for two categories namely (a) Debris-based experiments and (b) Non-Debris-based experiments are discussed in subsections VI-B and VI-C.

A. Controlled experiments

We conducted exhaustive experiments with *l*-Detect to study the detection of life at various ambient temperatures under a controlled environment. The ambient temperature range considered was 16° C – 32° C. For each data point, the behavior of the human skin temperature was studied. From our experiments, it is observed that when the ambient is between 22° C – 27° C, the skin temperature is between 30° C – 32° C. For higher ambient, we noticed that the skin temperature reaches a maximum of about 33° C. Furthermore, at temperatures between 16° C – 18° C, the skin temperature reduces considerably and is only a few degrees higher than the ambient, following the thermo-regulation of the body [30]. It is important to note that under debris, the whole body may not be visible to *l*-Detect. Before the data collection, the subjects were in the room for about 15 to 20 minutes to get adjusted to the room temperature. This is usually the case when a disaster strikes without prior warning. To mimic the real world, experiments were conducted with full as well as partial body parts exposed to *l*-Detect. Different postures such as crouching, sitting and standing were considered for data collection. Evaluations were carried out for all these postures at different ambient temperatures. The data was collected from various age groups with different body builds. Furthermore, data was collected for partially exposed human body parts like arms without cloth, arms with cloth, head, legs without cloth, legs with cloth, and torso. The isolation of body parts was done using a cardboard coffin. The *l*-Detect sensor system was placed at different distances between 0.5 m to 4.5 m in steps of 0.25 m from the subject.

B. Debris based experiments

Real-world scenarios include partially collapsed structures and debris. Our experiment included the subject's limb partially buried under the debris. We followed safety guidelines. The pictorial representation of the same is shown in Fig. 5 where a part of the arm and leg are exposed. The robotic toy

car with *l*-Detect was driven into the debris and moved around the subjects at different distances from 0.5 m to 2.25 m in steps of 0.25 m. For each distance, 50 sets of data were collected and tested to evaluate the detection probability.

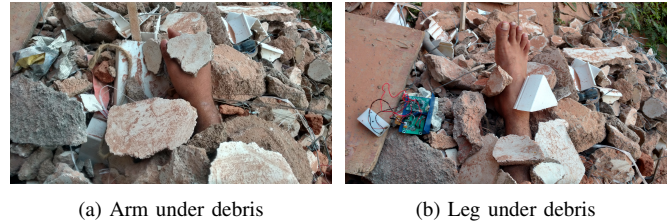


Fig. 5: Experiments in the debris environment (a) arm under a pile of debris; (b) leg under a pile of debris

Several false alarms and misdetections were observed in a debris environment, typically from exposed heated metal rods. Other false alarms include electronic gadgets, narrow beams of sunlight (causing concentrated heat spots), etc. as shown in Fig. 6. Our proposed algorithm was re-trained with these data to eliminate these false positives.



Fig. 6: Cases where thermal images can be interpreted incorrectly: (a) Air conditioning system; (b) Room heater; (c) Building's corridor; (d) Fluorescent lamp; (e) Outdoor view into trees and bushes. For (a), (b), and (d) due to a human-like thermal signature, a misdetection was recorded and was successfully filtered as too warm

C. Non-debris based experiments

Tests were conducted to evaluate the efficacy of *l*-Detect under a non-debris environment (outdoors, halls, corridors and rooms). The experiments included several miscellaneous objects like furniture, doors, electronic gadgets, etc. The data was collected with subjects in different postures at different places with varied distances from *l*-Detect.

Figures [7–10] depicts the second moment (SM) values of frames with and without humans in various postures at varying temperatures. Fig. 7 shows the results when the torso is exposed. The Y-axis indicates the SM and the X-axis is the distance between the subject and the *l*-Detect platform. The presence of life is most pronounced when the temperature differential is the highest. Fig. 8 shows the SMs when the head is exposed. In this scenario, the life is detected by *sm*Detect for temperatures up to 24° C, and for higher temperatures and distances beyond 1.25 m, *peak*Detect algorithm is used. Fig. 9 and Fig. 10 provide the SM for sitting and crouching

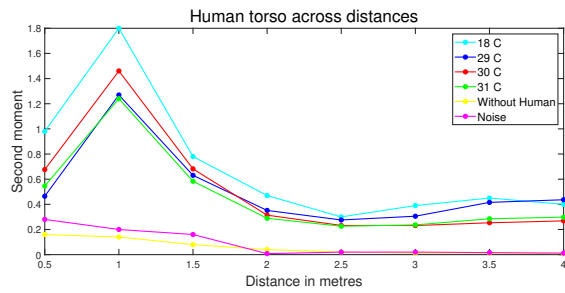


Fig. 7: Plot of human detection when only the torso is exposed across various distances and temperatures

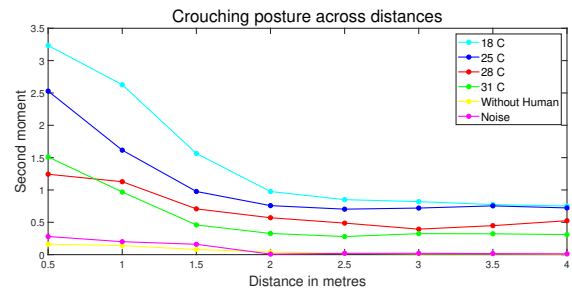


Fig. 10: Plot of human detection in crouching position at various distances and temperatures

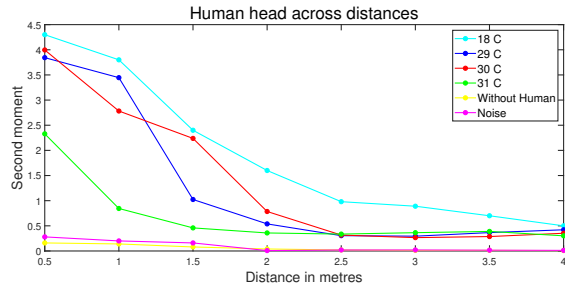


Fig. 8: Plot of human detection with only head exposed at various distances and temperatures

posture. Since more than 50% of the body is exposed to l -Detect the life detection probability is prominent. We also observed that with the increase in ambient temperature, the SM value with humans starts decreasing, making it challenging to differentiate between noise frames and human subject frames. Table III shows the detection probability achieved from the trained ML model for different body postures and parts with varied distances. The inference pattern from the ML model indicates a near 100% life detection up to the range of 2 m. Beyond 2 m, the detection probability reduces to around 90%. We also observed that the SM does not significantly vary between 2.0 to 4.0 m. Our experiments show that head and torso have good detection probability, followed by limb detection.

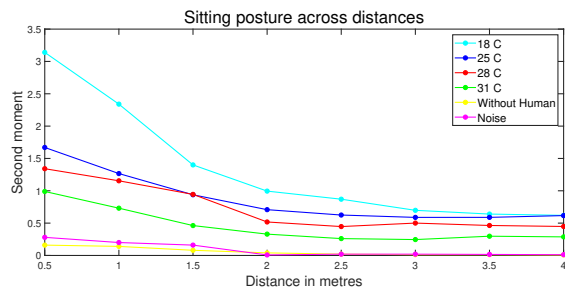


Fig. 9: Plot of human detection in sitting position at various distances and temperatures

TABLE III: Detection probability using SVM at ambient temperature of 25°C for different postures and distances

| Position/ Distance | Sitting | Crouching | Standing | Head | Torso | Limbs |
|-----------------------|---------|-----------|----------|------|-------|-------|
| 0.5 m | 100 | 100 | 100 | 100 | 100 | 100 |
| 1.0 m | 100 | 98 | 100 | 97 | 100 | 100 |
| 1.5 m | 99 | 98 | 100 | 92 | 93 | 95 |
| 2.0 m | 98 | 97 | 100 | 89 | 92 | 93 |
| 2.5 m | 98 | 97 | 100 | 89 | 87 | 88 |
| 3.0 m | 97 | 96 | 100 | 84 | 87 | 88 |
| 3.5 m | 94 | 95 | 100 | 77 | 88 | 88 |
| 4.0 m | 92 | 95 | 100 | 73 | 85 | 87 |
| 4.5 m | 90 | 94 | 100 | 72 | 73 | 72 |

VII. CONCLUSIONS

Many lives are lost in the aftermath of natural disasters because of a lack of capability to find survivors trapped under debris. There is difficulty in transporting equipment due to disruption in road infrastructure. Rescue workers systematically clear the debris looking for survivors. Since this is a time-consuming activity more lives are lost in the meanwhile. In this work, l -Detect aims to detect and notify the search and rescue team about the survivors trapped under debris. l -Detect is a thermopile sensor-based embedded system which is low-cost (around US \$30), lightweight (around 20 gm) with a small form factor, that can be mounted on any tiny robotic platform. Our embedded platform houses three simple algorithms including a machine learning inference model to detect life under debris. We characterize our sensor system for various scenarios, at different ambient temperatures. The exhaustive data collection and data evaluation of our system under close to real-life scenarios in varied ambient temperatures show that l -Detect can work over a wide range of temperatures between 16°C to 30°C. l -Detect is robust enough to detect humans with only partial exposure of human body parts. The detection probability is between the range of 85% to 100%. In cases when the ambient temperature is less than 25°C, the detection probability is close to 100% within a range of 1.5 m.

REFERENCES

- [1] A. R. Cross, "Moroccan Red Crescent Volunteers Helping Quake Survivors," American Red Cross, [Accessed: November 16, 2023]. [Online]. Available: <https://www.redcross.org/about-us/news-and-events/news/2023/teams-responding-after-earthquake-in-morocco.html>
- [2] T. Lewis, "On the Job: How Rescue Dogs Hunt for Tornado Survivors," May 2013. [Accessed: September 29, 2023]. [Online]. Available: <http://www.livescience.com/34552-rescue-dogs-hunt-for-tornado-survivors.html>
- [3] D. Linzmeier, M. Skutek, M. Mekhael, and K. Dietmayer, "A pedestrian detection system based on thermopile and radar sensor data fusion," in *Information Fusion, 2005 8th International Conference on*, vol. 2, July 2005, pp. 8 pp.–.
- [4] J. Honorato, I. Spiniak, and M. Torres-Torriti, "Human Detection Using Thermopiles," in *Robotic Symposium, 2008. LARS '08. IEEE Latin American*, Oct 2008, pp. 151–157.
- [5] R. Hahn, D. Lang, M. Haselich, and D. Paulus, "Heat mapping for improved victim detection," in *Safety, Security, and Rescue Robotics (SSRR), 2011 IEEE International Symposium on*, Nov 2011, pp. 116–121.
- [6] R. Shamroukh and F. Awad, "Detection of surviving humans in destructed environments using a simulated autonomous robot," in *Mechatronics and its Applications, 2009. ISMA '09. 6th International Symposium on*, March 2009, pp. 1–6.
- [7] K. Osuka, "On Development of Snake-like Robots to Search a Victim Left inside Debris," in *Robotics and Biomimetics, 2004. ROBIO 2004. IEEE International Conference on*, Aug 2004, pp. 65–69.
- [8] P. Rudol and P. Doherty, "Human Body Detection and Geolocalization for UAV Search and Rescue Missions Using Color and Thermal Imagery," in *Aerospace Conference, 2008 IEEE*, March 2008, pp. 1–8.
- [9] B.-D. Kang, K.-H. Jeon, D. Kyoung, S.-H. Kim, and J.-H. Hwang, "Multiple human body tracking using the fusion of CCD and thermal image sensor," in *Applied Imagery Pattern Recognition Workshop (AIPR), 2011 IEEE*, Oct 2011, pp. 1–4.
- [10] R. M. Narayanan, "Earthquake survivor detection using life signals from radar micro-doppler," in *Proceedings of the 1st International Conference on Wireless Technologies for Humanitarian Relief*, 2011, pp. 259–264.
- [11] M. Bao and X. Gao, "A Novel Life Signal Feature Extraction and Analysis Technique," in *2021 IEEE 4th International Conference on Electronics Technology (ICET)*. IEEE, 2021, pp. 817–822.
- [12] D. Shi, G. Gidion, L. M. Reindl, and S. J. Rupitsch, "Automatic Life Detection Based on Efficient Features of Ground-Penetrating Rescue Radar Signals," *Sensors*, vol. 23, no. 15, p. 6771, 2023.
- [13] K.-M. Chen, Y. Huang, J. Zhang, and A. Norman, "Microwave life-detection systems for searching human subjects under earthquake rubble or behind barrier," *Biomedical Engineering, IEEE Transactions on*, vol. 47, no. 1, pp. 105–114, Jan 2000.
- [14] F. Adib and D. Katabi, "See Through Walls with WiFi!" *SIGCOMM Comput. Commun. Rev.*, vol. 43, no. 4, pp. 75–86, Aug. 2013. [Online]. Available: <http://doi.acm.org/10.1145/2534169.2486039>
- [15] M. Zacharie and T. Shosaku, "Human only Made Life Signs Detection for Disaster Survivor Rescue," in *2021 6th International Conference on Intelligent Informatics and Biomedical Sciences (ICIIBMS)*, vol. 6. IEEE, 2021, pp. 274–278.
- [16] J. L. Honorato, I. Spiniak, and M. Torres-Torriti, "Human detection using thermopiles," in *2008 IEEE Latin American Robotic Symposium*. IEEE, 2008, pp. 151–157.
- [17] G. Hermosilla, J. Ruiz-del Solar, R. Verschae, and M. Correa, "Face recognition using thermal infrared images for Human-Robot Interaction applications: A comparative study," in *Robotics Symposium (LARS), 2009 6th Latin American*, Oct 2009, pp. 1–7.
- [18] F. Awad and R. Shamroukh, "Human detection by robotic urban search and rescue using image processing and neural networks," *International Journal of Intelligence Science*, vol. 2014, 2014.
- [19] D. Tanaka, J. Tanaka, K. Ikuru, Z. Liang, and I. Piumarta, "AkiKomi: Design and Implementation of a Mobile App System for Real-time Room Occupancy Estimation," in *2022 IEEE 11th Global Conference on Consumer Electronics (GCCE)*. IEEE, 2022, pp. 89–90.
- [20] V. Chidurala and X. Li, "Occupancy estimation using thermal imaging sensors and machine learning algorithms," *IEEE Sensors Journal*, vol. 21, no. 6, pp. 8627–8638, 2021.
- [21] C. Perra, A. Kumar, M. Losito, P. Pirino, M. Moradpour, and G. Gatto, "Monitoring indoor people presence in buildings using low-cost infrared sensor array in doorways," *Sensors*, vol. 21, no. 12, p. 4062, 2021.
- [22] J. Gao, X. Gao, W. Zhu, J. Zhu, and B. Wei, "Design and research of a new structure rescue snake robot with all body drive system," in *Mechatronics and Automation, 2008. ICMA 2008. IEEE International Conference on*, Aug 2008, pp. 119–124.
- [23] K. Osuka and H. Kitajima, "Development of mobile inspection robot for rescue activities: MOIRA," in *Intelligent Robots and Systems, 2003. (IROS 2003). Proceedings. 2003 IEEE/RSJ International Conference on*, vol. 4, Oct 2003, pp. 3373–3377 vol.3.
- [24] Fluke, "Fluke TI-10 IR Camera," 2023, <https://www.fluke.com/en-us/product/thermal-cameras/ti10/ds> [Accessed: November 16, 2023].
- [25] T. J. Seebeck, "Ueber die magnetische Polarisation der Metalle und Erze durch Temperaturdifferenz," *Annalen der Physik*, vol. 82, no. 3, pp. 253–286, 1826.
- [26] J. S. Warren, "Modern optical engineering: the design of optical systems," *McGraw-Hill, Inc., Figure*, vol. 14, p. 483, 1990.
- [27] N. Semiconductors, "nRF52840 Product Specification," 2023, https://infocenter.nordicsemi.com/pdf/nRF52840_PS_v1.7.pdf [Accessed: November 16, 2023].
- [28] Panasonic, "Grid-EYE Datasheet," 2023, <https://industrial.panasonic.com/cdbs/www-data/pdf/ADI8000/ast-ind-241606.pdf> [Accessed: November 16, 2023].
- [29] I. Syarif, A. Prügel-Bennett, and G. B. Wills, "SVM Parameter Optimization using Grid Search and Genetic Algorithm to Improve Classification Performance," *TELKOMNIKA Telecommunication Computing Electronics and Control*, vol. 14, pp. 1502–1509, 2016. [Online]. Available: <https://api.semanticscholar.org/CorpusID:64368789>
- [30] K. D. Stephan, "Radiometry before World War II: Measuring infrared and millimeter-wave radiation 1800–1925," *Antennas and Propagation Magazine, IEEE*, vol. 47, no. 6, pp. 28–37, 2005.